

# DISCRETE WAVELET FRAMES ON THE SPHERE

*I. Bogdanova and P. Vanderghelynst (1)*

*J.-P. Antoine, L. Jacques and M. Morvidone (2)*

(1) Signal Processing Institute (ITS), School of Engineering (FSTI), Swiss Federal Institute of Technology (EPFL)  
CH-1015 Lausanne, Switzerland  
email: {pierre.vanderghelynst, iva.bogdanova}@epfl.ch

(2) Institut de Physique Théorique (FYMA), Université Catholique de Louvain (UCL),  
B - 1348 Louvain-la-Neuve, Belgium.  
email: {antoine, ljacques, morvidon}@fy.ma.ucl.ac.be

## ABSTRACT

In this paper we exploit the Continuous Wavelet Transform (CWT) on the sphere introduced in [1, 2] to build the associated Discrete Wavelet Frames. We first explore half-continuous frames, i.e, frames where the position remains a continuous variable, and then move on to a fully discrete theory. This forces us to introduce the notion of controlled frames [5], which reflects the particular nature of the underlying theory, particularly the apparent conflict between dilation and the compactness of the  $S^2$  manifold. We conclude with some numerical illustrations and future work.

## 1. INTRODUCTION

Many examples in physics and medicine require the existence of suitable tools for analyzing data on spherical manifolds. As an analysing tool, the CWT has many advantages over the Fourier transform, namely a locality controlled by a dilation and a translation of the wavelet. Given the CWT, designing discrete spherical wavelet frames is of paramount importance and is the main contribution of this paper.

### 1.1 Continuous Wavelet Transform on the Sphere

The CWT on the sphere is based on affine transformations on the sphere, namely: rotations, defined by the element  $\rho$  of the group  $SO(3)$ ; and dilations, parametrized by the scale  $a \in \mathbb{R}_+^*$  [1]. If  $f \in L^2(S^2) \equiv L^2(S^2, d\mu)$ , with the rotation invariant measure on the sphere  $d\mu(\theta, \varphi) = \sin\theta d\theta d\varphi$ , we have the following unitary operators:

- rotation  $R_\rho (\rho \in SO(3))$ :

$$(R_\rho f)(\omega) = f(\rho^{-1}\omega), \quad \omega \equiv (\theta, \varphi). \quad (1)$$

- dilation  $D_a (a \in \mathbb{R}_+^*)$ :

$$(D_a f)(\omega) = \lambda(a, \theta)^{\frac{1}{2}} f(\omega_{1/a}), \quad (2)$$

where  $\omega_a \equiv (\theta_a, \varphi)$  with  $\tan \frac{\theta_a}{2} = a \tan \frac{\theta}{2}$ ;  $a > 0, \theta \in [0, \pi], \varphi \in [0, 2\pi]$ ; and  $\lambda$  is a normalization factor. This factor is given by

$$\lambda(a, \theta) = 4a^2 [(a^2 - 1) \cos \theta + (a^2 + 1)]^{-2}. \quad (3)$$

I.B. and P.V. acknowledge the support of the Swiss National Science Foundation through grant 200021-101880/1

M.M. acknowledges the financial support provided through the European Union's Human Potential Programme, under contract HPRN-CT-2002-00285 (HASSIP)

Intuitively, the action of dilation  $D_a$  on a function  $f \in L^2(S^2)$  corresponds to a Euclidean dilation of the function in the plane tangent the North Pole obtained by a stereographic projection from the South Pole, and lifted it back to the sphere by inverse stereographic projection. In the language of group theory, these two affine transformations, which do not generate a group neither commute, belong to the conformal group of the sphere  $S^2$  - the Lorentz group  $SO(3, 1)$ , where each subgroup is isolated using the Iwasawa decomposition (see [1] for details). Using these definitions, a square-integrable function  $\psi$  on  $S^2$  is called an *admissible wavelet* if there is a finite constant  $c \in \mathbb{R}_+^*$ , such that, for all  $l \in \mathbb{N}$ ,

$$G_\psi(l) = \frac{8\pi^2}{2l+1} \sum_{|m| \leq l} \int_{\mathbb{R}_+^*} \frac{da}{a^3} |\hat{\psi}_a(l, m)|^2 < c, \quad (4)$$

where  $\hat{\psi}_a(l, m) = \langle Y_l^m | \psi_a \rangle$  is the Fourier coefficient of  $\psi_a = D_a \psi$ . Even though this condition seems complicated and difficult to check, it can be proved that any admissible 2-D wavelet in  $\mathbb{R}^2$  yields an admissible spherical wavelet by inverse stereographic projection. In particular, for  $\phi(\theta, \varphi) = \exp(-\tan^2(\frac{\theta}{2}))$ , which is the inverse stereographic projection of a Gaussian on the sphere, a simple example of admissible wavelet is the *Difference of Gaussian (DOG)* spherical wavelet

$$\psi(\theta, \varphi) = \phi(\theta, \varphi) - \frac{1}{\alpha} [D_\alpha \phi](\theta, \varphi), \quad (5)$$

for  $\alpha \in \mathbb{R}_+^*$ .

Thus, with the given action of rotations and dilations, together with an admissible wavelet  $\psi \in L^2(S^2)$ , the CWT of a function  $f \in L^2(S^2)$  is:

$$W_f(\rho, a) = \langle \psi_{\rho, a} | f \rangle = \int_{S^2} d\mu(\omega) f(\omega) [R_\rho D_a \psi]^*(\omega). \quad (6)$$

This last expression is nothing else but a spherical correlation, i.e.,  $W_f(\rho, a) = (f * \psi_a^*)(\rho)$ .

The following proposition shows that the family of rotated and translated wavelets forms a continuous frame in  $L^2(S^2)$ , from which we derive a reconstruction formula:

**Proposition 1** *Let  $f \in L^2(S^2)$ . If  $\psi$  is an admissible wavelet such that  $\int_{S^2} d\mu \psi(\theta, \varphi) \neq 0$ , then*

$$f(\omega) = \int_{\mathbb{R}_+^*} \int_{SO(3)} \frac{dadv(\rho)}{a^3} W_f(\rho, a) [R_\rho L_\psi^{-1} D_a \psi](\omega), \quad (7)$$

where the coefficients are given by (6),  $L_\psi$  is the **frame operator** defined by

$$[\widehat{L_\psi h}](l, m) = G_\psi(l) \hat{h}(l, m), \quad \forall h \in L^2(S^2), \quad (8)$$

and  $G_\psi(l)$  is defined by (4).

The spherical CWT defines an approximate isometry, given by the following result :

**Corollary 1** *Under the condition of the previous proposition, the following Plancherel relation is satisfied*

$$\|f\|_2 = \int_{\mathbb{R}_+^*} \int_{SO(3)} \frac{d\text{ad}\nu(\rho)}{a^3} W_f(\rho, a) \tilde{W}_f^*(\rho, a) \quad (9)$$

with

$$\tilde{W}_f(\rho, a) = \langle \tilde{\psi}_{\rho, a} | f \rangle = \langle R_\rho L_\psi^{-1} D_a \psi | f \rangle. \quad (10)$$

The proof of these results and more details on the CWT on the sphere and its implementation can be found in [2]

Since the stereographic dilation is radial around the North Pole  $\eta \in S^2$ , an *axisymmetric* wavelet  $\psi$  on  $S^2$ , i.e., invariant under rotation around  $\eta$ , remains axisymmetric through dilation. So, if any rotation  $\rho \in SO(3)$  is decomposed in its Euler angles  $\varphi, \theta, \alpha \in S^1$ , i.e.,  $\rho = \rho(\varphi, \theta, \alpha)$ , then  $R_\rho \psi_a = R_{[\omega]} \psi_a$ , where  $[\omega] = \rho(\varphi, \theta, 0) \in SO(3)$  is the result of two consecutive rotations moving  $\eta$  to  $\omega = (\theta, \varphi) \in S^2$ . Consequently, the CWT is redefined on  $S^2 \times \mathbb{R}_+^*$  by

$$W_f(\omega, a) \equiv (f * \psi_a^*)([\omega]) \equiv (f * \psi_a^*)(\omega), \quad (11)$$

with  $a \in \mathbb{R}_+^*$ .

In that particular case, the reconstruction (9) becomes

$$f(\omega) = \int_{\mathbb{R}_+^*} \int_{S^2} \frac{d\text{ad}\mu(\omega')}{a^3} W_f(\omega', a) \tilde{\psi}_{\omega, a}(\omega'), \quad (12)$$

with  $\tilde{\psi}_{\omega, a} = R_{[\omega]} L_\psi^{-1} D_a \psi$ , and where  $L_\psi$  is the frame operator defined in (8) with  $G_\psi$  reducing to

$$G_\psi(l) = \frac{4\pi}{2l+1} \int_{\mathbb{R}_+^*} \frac{da}{a^3} |\hat{\psi}_a(l, 0)|^2. \quad (13)$$

## 2. DISCRETE WAVELET FRAMES ON THE SPHERE

In this section, we describe under which conditions the parameters of the continuous wavelet transform can be discretized. We focus on the case of axisymmetric wavelets.

### 2.1 Half-continuous Spherical Frame

#### 2.1.1 First Approach

We propose now to discretize the scale of the CWT on the sphere as we let the position vary continuously. In other words, we choose therefore

$$\omega \in S^2 \quad (14)$$

$$a \in A \equiv \{a_j \in \mathbb{R}_+^* : j \in \mathbb{Z}, a_j > a_{j+1}\} \quad (15)$$

which generate the half-continuous grid

$$\Lambda(A) = \{(\omega, a_j) : \omega \in S^2, j \in \mathbb{Z}\}. \quad (16)$$

In order to have a reconstruction of every function  $f \in L^2(S^2)$ , a first possible approach would be to impose

$$m \|f\|_2^2 \leq \sum_{j \in \mathbb{Z}} v_j \int_{S^2} d\mu(\omega) |W_f(\omega, a_j)|^2 \leq M \|f\|_2^2, \quad (17)$$

with  $m, M \in \mathbb{R}_+^*$  independent of  $f$ , and for some weights  $v_j > 0$  taking into account the discretization of the continuous measure  $\frac{da}{a^3}$ . In this case, the family

$$\{\psi_{\omega, a_j} = R_{[\omega]} D_{a_j} \psi : (\omega, a_j) \in \Lambda(m)\}, \quad (18)$$

constitutes a half-continuous frame in  $L^2(S^2)$ . The following proposition translates this last condition into the Fourier space (as identified by spherical harmonics).

**Proposition 2** *If there are two constants  $m, M \in \mathbb{R}_+^*$  such that*

$$m \leq \frac{4\pi}{2l+1} \sum_{j \in \mathbb{Z}} v_j |\hat{\psi}_{a_j}(l, 0)|^2 \leq M \quad (19)$$

for all  $l \in \mathbb{N}$ , then (17) is fulfilled.

Let us choose a DOG wavelet ( $\alpha = 1.25$ ) and a discretized dyadic scale with a certain number of voices  $K \in \mathbb{N}^0$ , namely

$$a_j = a_0 2^{-\frac{j}{K}}, \quad j \in \mathbb{Z}. \quad (20)$$

For the sake of simplicity, we replace the indices  $a_j$  by  $j$ . Moreover we choose weights  $v_j$  that take into account the discretization of the continuous measure  $\frac{da}{a^3}$ , which means

$$v_j = \frac{a_j - a_{j+1}}{a_j^3} = \frac{2^{\frac{j}{K}} - 1}{2^{\frac{1}{K}} a_j^2}. \quad (21)$$

We have estimated the bounds  $m$  and  $M$  respectively based on minimum and maximum of the quantity

$$S(l) = \frac{4\pi}{2l+1} \sum_{j \in \mathbb{Z}} v_j |\hat{\psi}_j(l, 0)|^2, \quad (22)$$

over  $l \in [0, 31]$  and for  $K \in [1, 4]$ . The results are shown in Table 1(a).

$K$	$m$	$M$	$M/m$
1	0.5281	0.9658	1.8288
2	0.6817	1.1203	1.8107
3	0.6537	1.1836	1.8107
4	0.6722	1.2171	1.8107

(a)

$K$	$m$	$M$	$M/m$
1	0.7313	0.7628	1.0431
2	0.8747	0.8766	1.0021
3	0.9242	0.9254	1.0014
4	0.9503	0.9512	1.0009

(b)

Table 1: Estimation of the bounds  $m$  and  $M$  as a function of the extremum of  $S(l)$  for some values of  $K$ . (a) First approach. (b) Second approach.

We can see that for  $K > 2$ , the relation  $M/m$  converges toward the value 1.8107. So, it does not converge toward a tight frame, for which  $m = M$ . This is mainly due to a non vanishing ‘‘gap’’ in the graph of  $S(l)$  for small values of  $l$ .

#### 2.1.2 Second Approach

Trying to converge to a tight frame, we adopt now a second approach for our half-continuous discretization. We start from the Plancherel relation as defined in Corollary 1. In other words, we will observe under which conditions we obtain a *controlled* frame [5]. That is, for two frame bounds  $m, M \in \mathbb{R}_+^*$ , we want

$$m \|f\|_2^2 \leq \sum_{j \in \mathbb{Z}} v_j \int_{S^2} d\mu(\omega) |W_f \tilde{W}_j^*(\omega, a_j)|^2 \leq M \|f\|_2^2, \quad (23)$$

where  $f \in L^2(S^2)$ ,  $\tilde{W}_f(\omega, a_j) = \langle R_{[\omega]} L_\psi^{-1} D_a \psi | f \rangle$ , and where the brackets mean multiplication of two functions. The operator  $L_\psi$  controls the frame and it is bounded with bounded inverse if and only if the wavelet  $\psi$  is admissible.

**Proposition 3** *If there exist two constants  $m, M \in \mathbb{R}_+^*$  such that*

$$m \leq \frac{4\pi}{2l+1} G_\psi(l)^{-1} \sum_{j \in \mathbb{Z}} v_j |\hat{\psi}_j(l, 0)|^2 \leq M, \quad (24)$$

with  $G_\psi(l)$  given by (13) and for all  $l \in \mathbb{N}$ , then (23) is verified.

By using the same scale discretization, the same wavelet and the same weights  $v_j$  as in the first approach, we find now (see Table 1(b)) that for  $l \in [0, 31[$ , the ratio  $M/m$  tends to 1 as  $K$  increases. A tight frame is thus reachable by considering the controlled frame approach.

### 2.1.3 Construction of a tight half-continuous frame

It is possible to build a tight half-continuous frame on the sphere using the previous considerations.

**Proposition 4** *Let  $\{a_j : j \in \mathbb{Z}, a_j > a_{j+1}\}$  be a sequence of scales. If  $\psi$  is an axisymmetric wavelet such that*

$$g_\psi(l) = \frac{4\pi}{2l+1} \sum_{j \in \mathbb{Z}} v_j |\hat{\psi}_j(l, 0)|^2 \neq 0, \quad \forall l \in \mathbb{N}, \quad (25)$$

then,

$$f(\omega) = \sum_{j \in \mathbb{Z}} v_j [W_f(\cdot, a_j) \star \psi_j^\#](\omega), \quad (26)$$

with  $\psi_j^\# = l_\psi^{-1} D_{a_j} \psi$  and  $l_\psi$  is an operator defined in the Fourier domain by  $\widehat{l_\psi^{-1} h}(l, m) = g_\psi^{-1}(l) h(l, m)$ . In other words, the frame controlled by  $l_\psi$  is tight.

The new operator  $l_\psi$  is nothing else but the discretization of  $L_\psi$  defined in (13).

Notice that a scaling function  $\zeta$  s.t.

$$|\hat{\zeta}(l, m)|^2 = \delta_{m,0} \sum_{j=-\infty}^{-1} v_j |\hat{\psi}_j(l, 0)|^2. \quad (27)$$

can be introduced so that

$$f(\omega) = [S_f \star \zeta^\#](\omega) + \sum_{j \in \mathbb{N}} v_j [W_f(\cdot, a_j) \star \psi_j^\#](\omega), \quad (28)$$

with  $S_f(\omega) = \langle R_{[\omega]} \zeta | f \rangle$  and  $\zeta^\# = l_\psi^{-1} \zeta$ .

## 2.2 Discrete Spherical Frames

In this section, we will completely discretize the CWT on the sphere. The scales are discretized as previously, namely

$$a \in A = \{a_j \in \mathbb{R}_+^* : a_j > a_{j+1}, j \in \mathbb{Z}\}, \quad (29)$$

and the positions are taken in an equi-angular grid  $\mathcal{G}_j$  indexed by the scale level, related to the scale in such a way that  $\omega \in \mathcal{G}_j$ , with

$$\mathcal{G}_j = \{(\theta_{jp}, \varphi_{jq}) \in S^2 : \theta_{jp} = \frac{(2p+1)\pi}{4B_j}, \varphi_{jq} = \frac{q\pi}{B_j}\}, \quad (30)$$

$p, q \in \mathcal{N}_j \equiv \{n \in \mathbb{N} : n < 2B_j\}$  and for some range of bandwidth  $B = \{B_j \in 2\mathbb{N}, j \in \mathbb{Z}\}$ . Actually,  $\theta_{jp}$  form a pseudo-spectral grid and are localized on the knots of a Chebishev polynomial of order  $2B_j$  [3, 4]. With this choice, for certain weights  $w_{jp} > 0$  and on every grid  $\mathcal{G}_j$ , the following quadrature rule is verified [4]

$$\int_{S^2} d\mu(\omega) f(\omega) = \sum_{p, q \in \mathcal{N}_j} w_{jp} f(\omega_{jpq}), \quad (31)$$

with  $\omega_{jpq} = (\theta_{jp}, \varphi_{jq})$  and for every band-limited function  $f \in L^2(S^2)$  of bandwidth  $B_j$ , i.e., such that  $\hat{f}(l, m) = 0$  for all  $l \geq B_j$ .

The complete space of discretization is finally

$$\Lambda(A, B) = \{(a_j, \omega_{jpq}) : j \in \mathbb{Z}, p, q \in \mathcal{N}_j\}. \quad (32)$$

In this case, for an axisymmetric and admissible mother wavelet  $\psi \in S^2$ , the family of wavelets

$$\{\psi_{jpq} = R_{[\omega_{jpq}]} D_{a_j} \psi : j \in \mathbb{Z}, p, q \in \mathcal{N}_j\} \quad (33)$$

constitutes a weighted frame controlled by the operator  $L_\psi$ , if there exist two constants  $m, M \in \mathbb{R}_+^*$  such that, for any function  $f \in L^2(S^2)$ , we have

$$m \|f\|_2^2 \leq \sum_{j \in \mathbb{Z}} \sum_{p, q \in \mathcal{N}_j} v_j w_{jp} [W_f \tilde{W}_f^*](\omega_{jpq}, a_j) \leq M \|f\|_2^2, \quad (34)$$

In the last expression, the values  $v_j w_{jp}$  replace the measure  $\frac{d\mu}{d\Omega}(\theta, \varphi)$ .

**Proposition 5** *Let the discretized grid  $\Lambda(A, B)$  be given as in (32). Let  $\psi$  be an axisymmetric and admissible wavelet on  $S^2$ , and*

$$S'(l) = \sum_{j \in \mathbb{Z}} \frac{4\pi v_j}{2l+1} \mathbb{1}_{[0, B_j[}(l) G_\psi^{-1}(l) |\hat{\psi}_j(l, 0)|^2, \quad (35)$$

$$\delta = \|\mathcal{X}\| \equiv \sup_{(H_l)_{l \in \mathbb{N}}} \frac{\|\mathcal{X}H\|}{\|H\|}, \quad (36)$$

with the infinite matrix  $(\mathcal{X}_{l'l'})_{l, l' \in \mathbb{N}}$  s.t.

$$\mathcal{X}_{l'l'} = \sum_{j \in \mathbb{N}} c_j(l, l') \mathbb{1}_{[2B_j, +\infty[}(l+l') |\hat{\psi}_j(l, 0)| |\hat{\psi}_j(l', 0)| \quad (37)$$

and  $c_j(l, l') = \frac{2\pi v_j}{B_j} G_\psi^{-1}(l) [(2(l+B_j)+1)(2(l'+B_j)+1)]^{\frac{1}{2}}$ .

If we have

$$0 \leq \delta < K_0 \leq K_1 < \infty, \quad (38)$$

with  $K_0 = \inf_{l \in \mathbb{N}} S'(l)$  and  $K_1 = \sup_{l \in \mathbb{N}} S'(l)$ , then the family (33) is a weighted spherical frame controlled by the operator  $L_\psi$  with frames bounds  $K_0 - \delta, K_0 + \delta$ .

A detailed proof of this proposition can be found in [5].

The evaluation of  $\|\mathcal{X}\|$  could be complex when the size of  $\mathcal{X}$  is infinite. However, in practice, we work with band-limited functions  $f \in L^2(S^2)$  of bandwidth  $b \in \mathbb{N}^0$ . Consequently,  $\|\mathcal{X}\|$  could be changed by the norm of the finite matrix  $(\mathcal{X}_{l'l'})_{0 \leq l, l' < b}$ .

We have estimated the bounds of a spherical DOG wavelet frame in the case  $b = 64$ , using a dyadically discretized scale (with  $K = a_0 = 1$  in (20)), while the bandwidth, associated to the grid size supporting each resolution  $j$ , was fixed to

$$B_j = B_0 2^{|j|}, \quad B_0 \in \mathbb{N}, \quad (39)$$

where  $B_0$  is the minimal bandwidth associated to  $\psi_1$ . The last equation takes into account the particular nature of the stereographic dilation on  $S^2$ . Indeed, for the DOG wavelet, we may show that the (essential) support of  $\hat{\psi}_j$  increases with  $j$  if  $j > 0$ , and grows with  $-j$  if  $j \leq 0$  [5].

Table 2 presents the results of the evaluation of  $K_0$ ,  $K_1$  and  $\delta$  as well as the bounds of the associated frames.

	$K_0$	$K_1$	$\delta$	$m = K_0 - \delta$	$M = K_1 + \delta$	$M/m$
$B_0 = 2$	0.6807	0.7700	84.1502	—	—	—
$B_0 = 4$	0.7402	0.7790	0.0594	0.6808	0.8384	1.2314
$B_0 = 8$	0.7402	0.7790	0.0014	0.7388	0.7804	1.0564

Table 2: Evaluation of  $K_0$ ,  $K_1$  and  $\delta$  on the functions  $f \in L^2(S^2)$  at bandwidth 64.

One can see that for  $B_0 \geq 4$ , condition (38) is reached. A tight frame cannot be obtained while we increase  $B_0$ . Actually, if  $B_0$  tends to infinity, the spherical grids at each resolution get finer and finer and we approach the half-continuous frames, but as seen in the previous section, the one voice discretization of the scale is not sufficient.

### 3. EXAMPLES AND IMPLEMENTATIONS

The next application shows the advantages of the half-continuous frame decomposition over methods constructed completely in the frequency domain. We work on a cartography of the surface of Jupiter and we would like to locally enhance the details in a neighborhood of its “red spot”. All the spherical correlations defining the wavelet coefficients and the reconstruction (28) have been performed in Fourier space using the spherical correlation theorem [4]

$$\widehat{f \star g}(l, m) = \sqrt{\frac{4\pi}{2l+1}} \hat{f}(l, m) \hat{g}(l, 0), \quad (40)$$

for  $f \in L^2(S^2)$  and for any axisymmetric function  $g \in L^2(S^2)$ , and by using the SpharmonicKit [6] which performs fast (forward and inverse) spherical harmonics transforms. All these methods are integrated into the Matlab©YAWtb toolbox<sup>1</sup>.

We consider an equi-angular grid of size is  $512 \times 512$  and the data bandwidth is set to  $b = 256$ . In this context the DOG wavelet is properly discretized for a scale range with  $|j| \leq 7$  and  $a_0 = 1$ .

We proceed as follows: before reconstruction the coefficients at the finer scale  $W_f(\omega, a_7)$  are multiplied by a mask function that increases their amplitudes in a vicinity of the red spot. The rest of the coefficients are not modified.

Results after reconstruction are shown in Figure 1. We show a zoom over the red spot of the reconstructed signal without any processing (left) and the modified version where the red spot’s details are clearly sharper (right).

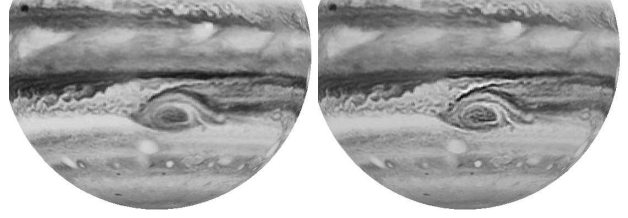


Figure 1: Enhancement of the details of Jupiter’s red spot: zoom over the spot (left); zoom over the spot with sharper details (right).

### 4. CONCLUSIONS AND FUTURE WORK

Conditions on the existence of half-continuous and discrete spherical frames have been established from the (stereographic) spherical CWT [1]. The last section illustrates the efficiency of a particular DOG (half-continuous) tight frame with a simple Jovian image enhancing. An example of a discrete frame using the results of Proposition 5 has still to be designed. These techniques could serve for instance to discover the Gaussian anisotropies in the astronomical *Cosmic Microwave Background* [7], or to track the orientations in  $\mathbb{R}^3$  of fibre in the human brain connectivity [8]. Work in these directions is currently in progress.

### REFERENCES

- [1] J-P. Antoine and P. Vandergheynst, “Wavelets on the 2-Sphere: a Group Theoretical Approach,” *Appl. Comput. Harmon. Anal.*, vol. 7, pp. 1–30, Aug. 1999.
- [2] J-P. Antoine, L. Demanet, L. Jacques and P. Vandergheynst, “Wavelets on the Sphere: Implementations and Approximations,” in *Appl. Comput. Harmon. Anal.*, vol. 13, pp. 177–200, 2001.
- [3] J. Boyd, *Chebyshev and Fourier Spectral Method*. 49 of Lecture Notes in Engineering, Springer, Verlag 1989.
- [4] J. R. Driscoll and D.M. Healy, “Computing Fourier Transform and Convolutions on the 2-Sphere,” *Advances in Applied Mathematics*, vol. 15, pp.202–455,1994.
- [5] I. Bogdanova, P. Vandergheynst, L. Jacques, M. Morvidone, J.-P. Antoine, “Stereographic Frames of Wavelets on the Sphere,” *ITS Technical Report No. 2004.001*.
- [6] D. Rockmore, S. Moore, D. Healy and P. Kostelec, “SpharmonicKit: C Toolkit doing Fast Legendre and Scalar Spherical Transforms,” <http://www.cs.dartmouth.edu/~geelong/sphere/>.
- [7] E. Martinez-Gonzalez, J.E. Gallegos, F. Argueso, L. Cayon, and J.L. Sanz, “The performance of spherical wavelets to detect non-Gaussianity in the CMB sky,” *Mon. Not. R. Astron. Soc.*, vol. 336, pp.22–32, 2002.
- [8] P. Hagmann, J. Thiran, L. Jonasson, P. Vandergheynst, S. Clarke, P. Maeder, and R. Meuli, “Dti mapping of human brain connectivity: statistical fibre tracking and virtual dissection,” *Neuroimage*, vol. 19(3), pp.545–554, July 2003.

<sup>1</sup>Developed by some of us and freely (GPLy) available at <http://www.fyma.ucl.ac.be/projects/yawtb>.